Robust Nonlinear Control-Based Trajectory Tracking for Quadrotors Under Uncertainty

Krishna Bhavithavya Kidambi, *Member, IEEE*, Cornelia Fermüller, *Member, IEEE*, Yiannis Aloimonos, *Senior Member, IEEE*, and Huan Xu, *Member, IEEE*

***Abstract*—This letter presents a modified robust integral of signum error (RISE) nonlinear control method, for quadrotor trajectory tracking and control. The proposed control algorithm tracks trajectories of varying speeds, uncertainties and disturbance magnitudes. The control law presented achieves asymptotic regulation of the quadrotor states in the presence of parametric uncertainties and disturbances. To achieve the results, first the quadrotor UAV dynamics are derived in a strict form. Then, a robust state feedback control is developed in both the position and attitude loop respectively. A detailed Lyapunov-based stability analysis is provided which proves the proposed control method theoretically guarantees asymptotic regulation of the quadrotor states. To illustrate the performance of the proposed control method, comparative numerical simulation results are provided, which demonstrate an improved performance under varying disturbance and uncertain magnitudes.**

***Index Terms*—Robust control, autonomous vehicles, control applications.**

I. Introduction

QUADROTORS have been a topic of extensive research over the past decade with applications in military and civilian domains, such as surveillance and agriculture [1], [2]. Quadrotors are highly nonlinear and strongly coupled, underactuated dynamic systems. The dynamics of the quadrotor consist of two loops, an outer (position) loop and an inner (attitude) loop. One of the challenging problems is how to effectively control the quadrotor trajectory in three dimensional space.

Initial research in quadrotor control focused on linearizing the nonlinear quadrotor dynamics around an operating point using classical control techniques such as proportional-integral-derivative PID [3], [4], proportional-derivative (PD) [5], and linear quadratic regulators (LQR) [6]. In [3], multiple PID controllers were developed to control the quadrotor system. A pilot augmentation control system was developed in [4], with a double lead compensator for the inner loop controller and a pure proportional controller for the outer loop. A unified LQR control of rotational and translational states under time-varying system dynamics was proposed in [6]. PID control are attractive because of their ease of implementation and are desirable in practical autopilot design. However, the strong coupling and intrinsic nonlinearities inherent in the quadrotor dynamics combined with the cumbersome approach of gain tuning pose several limitations. To overcome these limitations, a variety of nonlinear control strategies have been proposed in the literature over the years. Generally, nonlinear control methods achieve admissible performance under uncertain environmental conditions, thus enabling accurate tracking and aggressive maneuvering. They also increase the stability basin of attraction. Many nonlinear control algorithms have been developed for quadrotors over the years, such as feedback linearization (FL) [7], [8], back stepping [9], [10], optimal control [11], adaptive control [12], [13], sliding mode control (SMC) [14], [15], and robust control [16].

The feedback linearization technique presented in [7] is mathematically convenient and has ease of implementation. But the control technique is sensitive to external disturbances and model uncertainties. In [8], using feedback linearization, a linear control law is designed to achieve a desired formation. In addition, a sliding mode compensator had to be designed to account for possible errors during feedback linearization. Backstepping like subcontrollers are synthesized in [9] for constraint-based quadrotor trajectory tracking. In [11] a linear quadratic integral optimal control is presented, however feedback linearization has been used to deal with the nonlinearity of the quadrotor dynamics. A nonlinear adaptive state feedback controller is presented in [12] in the presence of forced disturbances, but the basin of attraction is restricted to a set of initial conditions. An adaptive dynamic control structure comprising a kinematic controller and a dynamic compensator for quadrotor trajectory tracking is presented in [13].

Manuscript received September 16, 2020; revised November 23, 2020; accepted December 9, 2020. Date of publication December 15, 2020; date of current version March 26, 2021. This work was supported in part by ONR under Grant N00014-17-1-2622; and in part by the National Science Foundation under Grant BCS 1824198. Recommended by Senior Editor L. Menini. *(Corresponding author: Krishna Bhavithavya Kidambi.)*

Krishna Bhavithavya Kidambi, Cornelia Fermüller, Yiannis Aloimonos are with the Perception and Robotics Group, University of Maryland, College Park, MD 20742 USA (e-mail: kidambi@umd.edu; fer@umiacs.umd.edu; yiannis@cs.umd.edu).

Huan Xu is with the Department of Aerospace Engineering, Institute for Systems Research, University of Maryland, College Park, MD 20742 USA (e-mail: mumu@umd.edu).

Digital Object Identifier 10.1109/LCSYS.2020.3044833

With rapidly increasing advancements in control techniques for quadrotors, robust control approaches have gained considerable attention from the control community to address the problem of uncertainties and disturbances. One among these is robust integral of signum error (RISE) control, first proposed in [17], which is continuous and can achieve asymptotic stability in the presence of bounded disturbances and model uncertainties [18]–[21]. However, in order to mitigate the model uncertainties, conservative high feedback gains are required to achieve precision tracking. Reference [18] describes a neural network (NN)-based linear dynamic inversion (LDI) with RISE feedback for the inner loop and a LDI with RISE feedback for the outer loop. An approach using adaptive RISE feedback controllers for both the inner and outer loop is presented in [19]. A method for quadrotor trajectory tracking has been presented in [20], which uses a NN-based PD-SMC method for the outer loop and a RISE method for the inner loop. In [21], an integral model predictive control is presented along with a nonlinear $\mathcal{H}_\infty$ controller for quadrotor trajectory tracking in the presence of aerodynamic disturbances and 30% structural uncertainties.

The contribution of this letter is a modified RISE-based feedback control strategy for quadrotor trajectory tracking under varying levels of uncertainties and external disturbances. Traditional RISE formulation consists of a signum of error ($sgn(e)$) term in the control expression, but this modified RISE control contains signum of rate of error ($sgn(r)$). The presence of this new term in the control structure makes it more robust to varying levels of parametric uncertainties, disturbance magnitudes and the control algorithm can track trajectories of varying speeds. Apart from the aforementioned advantages, the control structure does not require additional gain tuning under varying disturbance magnitudes and uncertainties. The design of the proposed controller is divided into an inner (attitude) loop and an outer (position) loop. The proposed control algorithm could be used in civilian applications like package delivery or in fire fighting drones or even in future commercial transportation applications. Both the inner and outer loop control structure are based on modified RISE. The main contributions of the letter are summarized as:

1) A fundamentally modified RISE control structure for both the outer and inner loop for quadrotor dynamic systems is provided. The biggest advantage of the proposed control structure is it tracks prefined trajectories at varying speeds and disturbance magnitudes. The algorithms also accounts for varying levels of uncertainty (0%-30%) with little or no gain tuning.
2) Closed-loop stability of the quadrotor dynamic system is shown using Lyapunov stability theory, which provides theoretical guarantees on the closed loop performance and proves that the closed-loop system achieves asymptotic regulation of the quadrotor states in the presence of uncertainties and disturbances.
3) The proposed theoretical contributions are validated through numerical simulations to demonstrate proof of concept numerically.

The rest of this letter is organized as follows: Section II describes the nonlinear 6-DOF dynamic model of the quadrotor. The design procedure for the modified RISE-based trajectory tracking controller is given in Section III, with the outer loop in Section III-A and the inner loop in Section III-B, respectively. In Section IV, the closed-loop stability analysis is presented. Numerical simulations demonstrate the effectiveness of the proposed method are provided in Section V followed by conclusions in Section VI.

II. Dynamic Model

The nonlinear dynamics of a quadrotor is well known in the literature [22], [23]. Neglecting the effects of rotor dynamics, gyroscope and blade flapping on the complete system dynamics, the explicit form of the dynamics with position and orientation can be written as [23]

$$m\ddot{\Lambda} = -K_1\dot{\Lambda} - \mathcal{G} + G_1U_1 + d_\Lambda(t) \tag{1}$$

$$J\ddot{\Gamma} = -K_2\dot{\Gamma} + G_2U_2 + d_\Gamma(t) \tag{2}$$

where $m \in \mathbb{R}^+$ is the mass of the quadrotor, $\Lambda = [x, y, z]^T$ and $\Gamma = [\phi, \theta, \psi]^T$ denote the position and Euler angles defined in the inertial frame and body frame, respectively. The control input $U_1 \in \mathbb{R}$ denotes the applied thrust, and $U_2 = [u_\phi, u_\theta, u_\psi]^T$ denotes the torque along x, y, z axis, respectively. $\mathcal{G} = [0, 0, mg]^T$, where g = 9.81 ms^{-2} is the gravitational acceleration, $J = diag(J_1, J_2, J_3)^T \in \mathbb{R}^{3\times3}$ is a positive definite diagonal moment of inertia matrix. $K_1 = diag(k_x, k_y, k_z) \in \mathbb{R}^{3\times3}, K_2 = diag(k_\phi, k_\theta, k_\psi) \in \mathbb{R}^{3\times3}$ are the damping matrices. $G_1 = [c(\psi)s(\theta)c(\phi) + s(\psi)s(\phi), s(\phi)s(\theta)c(\psi) - c(\psi)s(\phi), c(\theta)c(\phi)]^T \in \mathbb{R}^{3\times1}$ is the position subsystem related to orientation with $c(\cdot), s(\cdot)$ denoting $cos(\cdot)$ and $sin(\cdot)$. $G_2 = diag(l, l, c) \in \mathbb{R}^{3\times3}$ with l the distance from each rotor to the center of the mass of the quadrotor and c a constant force to moment ratio. $d_\Lambda(t), d_\Gamma(t)$ are the external disturbances, bounded unmodeled dynamics in the rotational dynamics.

In the subsequent control design section, the original dynamics are transformed into the following notation for the sake of simplicity,

$$\dot{X_1} = X_2 \tag{3}$$

$$\dot{X_2} = f_1(X_2) + u_1 + d_2(t) \tag{4}$$

$$\dot{X_3} = X_4 \tag{5}$$

$$\dot{X_4} = f_2(X_4) + g_4u_2 + d_4(t) \tag{6}$$

where $X_1 = \Lambda$, $X_2 = \dot{\Lambda}$, $X_3 = \Gamma$ and $X_4 = \dot{\Gamma}$.

$$f_1(X_2) = -\frac{\bar{K_1}\dot{\Lambda}}{m}; \quad u_1 = \frac{-\mathcal{G} + G_1U_1}{m} \tag{7}$$

$$f_2(X_4) = -J^{-1}\bar{K_2}\dot{\Gamma}; \quad g_4 = J^{-1}G_2 \tag{8}$$

$$d_2(t) = \frac{d_\Lambda(t) - K_{1\Delta}\dot{\Lambda}}{m}; \quad d_4(t) = J^{-1}[K_{2\Delta}\dot{\Gamma} + d_\Gamma(t)]$$

$$m = \bar{m} + m_\Delta; \quad J = \bar{J} + J_\Delta$$

$$K_1 = \bar{K_1} + K_{1\Delta}; \quad K_2 = \bar{K_2} + K_{2\Delta}$$

where $\bar{(\cdot)}$ denotes the nominal values and $(\cdot)_\Delta$ denotes the uncertainty associated with respective parameters. d_2 and d_4 are the disturbances in the position and attitude loops.

III. Control Development

A. Outer Loop

The control objective is, to regulate the system to track a given sufficiently smooth, time varying reference trajectory despite the presence of structured and unstructured uncertainties in the dynamic model. Thus, the control objective can be mathematically stated as

$$\|e(t)\| \to 0 \tag{9}$$

where $\|.\|$ in (9) denotes standard Euclidean norm. To quantify the control objective and to facilitate the subsequent stability analysis, the tracking error $e_1(t)$ and auxiliary tracking errors $e_2(t), r_1(t)$ for the position loop are defined as

$$e_1 = X_1 - X_{1d} \in \mathbb{R}^3 \tag{10}$$

$$e_2 = \dot{e}_1 + \alpha_1 e_1 \in \mathbb{R}^3; \quad r_1 = \dot{e}_2 + \alpha_2 e_2 \in \mathbb{R}^3, \tag{11}$$

where $\alpha_1, \alpha_2 \in \mathbb{R}$ denote positive control gains. Taking the derivative of (11) and using the definition in (3) and (4), the open loop error dynamics can be expressed as

$$\dot{r}_1 = \dot{f}_1(X_2) + \dot{u}_1(t) + \dot{\Delta}_1 u_1(t) + \dot{d}_2(t) - \dddot{X}_{1d} + \alpha_1 \ddot{e}_1 + \alpha_2 \dot{e}_2. \tag{12}$$

The error dynamics in (12) can be expressed as

$$\dot{r}_1 = \tilde{N}_1(t) + N_{1d} + \dot{u}_1(t) + \dot{\Delta}_1(t) u_1(t) - e_2, \tag{13}$$

where the unknown auxiliary functions, $\tilde{N}_1(t), N_{1d}(t) \in \mathbb{R}^3$ are defined as

$$\tilde{N}_1(t) = \dot{f}_1(X_2) + +\alpha_1 \ddot{e}_1 + \alpha_2 \dot{e}_2 + e_2; \quad N_{1d} = \dot{d}_2(t) - \dddot{X}_{1d}. \tag{14}$$

Assumption 1: The disturbances are slowly (sufficiently) time-varying and approximate model knowledge is available such that $\dot{\Delta}_1(t)$ satisfies

$$\left\| \dot{\Delta}_1(t) \right\|_{i\infty} < \epsilon_1 < 1, \tag{15}$$

where $\epsilon_1 \in \mathbb{R}^+$ is a known bounding constant, and $\| \cdot \|_{i\infty}$ denotes the induced infinity norm.

1) Closed-Loop Error System: Based on the open-loop error system dynamics in (12), the control term $u_1(t)$ is designed as:

$$\dot{u}_1(t) = -k_{u1} \|u_1(t)\| sgn(r_1) - (k_{s1} + 1) r_1 - \beta_1 sgn(r_1), \tag{16}$$

where $k_{u1}, k_{s1}, \beta_1 \in \mathbb{R}$ are positive, control gains. After substituting (16) into (13), the closed-loop error dynamics is obtained as

$$\dot{r}_1 = \tilde{N}_1 + N_{1d} - k_{u1} \|u_1(t)\| sgn(r_1) - (k_{s1} + 1) r_1 - \beta sgn(r_1) + \dot{\Delta}(t) u_1(t) - e_2. \tag{17}$$

B. Inner Loop

The tracking error in the orientation loop is defied as

$$e_3 = X_3 - X_{3d}, \tag{18}$$

where $X_{3d} = [\phi_d, \theta_d, \psi_d]^T \in \mathbb{R}^3$. The desired attitude ψ_d is a user defined signal and the remaining two desired orientation signals ϕ_d, θ_d are defined using the following equations [24]:

$$\phi_d = sin^{-1}\left[\frac{m}{U_1} (u_1 sin(\psi_d) - u_2 cos(\psi_d)) \right], \tag{19}$$

$$\theta_d = tan^{-1}\left[\frac{1}{(u_3 + g)} (u_1 cos(\psi_d) + u_2 cos(\psi_d)) \right], \tag{20}$$

where U_1 is the thrust force, which is defined as

$$U_1 = m\sqrt{u_1^2 + u_2^2 + (u_3 + g)^2}. \tag{21}$$

The auxiliary tracking errors $e_4(t)$ and $r_2(t)$ are defined as

$$e_4 = \dot{e}_3 + \alpha_3 e_3 \in \mathbb{R}^3; \quad r_2 = \dot{e}_4 + \alpha_4 e_4 \in \mathbb{R}^3, \tag{22}$$

where $\alpha_3, \alpha_4 \in \mathbb{R}$ denote positive control gains. Taking the derivative of (22) and using the definition in (5) and (6), the open loop error dynamics of the orientation loop can be expressed as

$$\dot{r}_2 = \dot{f}_2(X_4) + \dot{u}_2(t) + \dot{\Delta}_g(t) u_2(t) + \dot{d}_4(t) - \dddot{X}_{3d} + \alpha_3 \ddot{e}_3 + \alpha_4 \dot{e}_4. \tag{23}$$

The error dynamics in (23) can be expressed as

$$\dot{r}_2 = \tilde{N}_2(t) + N_{2d} + \dot{u}_2(t) + \dot{\Delta}_g(t) u_2(t) - e_4. \tag{24}$$

Assumption 2: The disturbances are slowly time-varying and approximate model knowledge is available such that the uncertain $\dot{\Delta}_g(t)$ satisfies

$$\left\| \dot{\Delta}_g(t) \right\|_{i\infty} < \epsilon_2 < 1, \tag{25}$$

where $\varepsilon_2 \in \mathbb{R}^+$ is a known bounding constant, and $\| \cdot \|_{i\infty}$ denotes the induced infinity norm.

The unknown auxiliary functions, $\tilde{N}_2(t), N_{2d}(t) \in \mathbb{R}^3$ are defined as:

$$\tilde{N}_2(t) = \dot{f}_2(X_4) + \alpha_3 \ddot{e}_3 + \alpha_4 \dot{e}_4 + e_4; \quad N_{2d} = \dot{d}_4(t) - \dddot{X}_{3d}. \tag{26}$$

The motivation for the separation of terms in (14) and (26) are based on the fact that the following inequalities can be developed

$$\|\tilde{N}_1\| \le \rho_1(\|z_1\|)\|z_1\|, \quad \|N_{1d}\| \le \zeta_{N_{1d}}, \quad \|\dot{N}_{1d}\| \le \zeta_{\dot{N}_{1d}} \tag{27}$$

$$\|\tilde{N}_2\| \le \rho(\|z_2\|)\|z_2\|, \quad \|N_{2d}\| \le \zeta_{N_{2d}}, \quad \|\dot{N}_{2d}\| \le \zeta_{\dot{N}_{2d}} \tag{28}$$

where $\zeta_{N_{1d}}$, $\zeta_{\dot{N}_{1d}}$,$\zeta_{N_{2d}}$ and $\zeta_{\dot{N}_{2d}} \in \mathbb{R}^+$ are known bounding constants; $\rho_1(\cdot)$, $\rho_2(\cdot)$ are positive, globally invertible, non-decreasing function; $z_1(t), z_2(t) \in \mathbb{R}^9$ respectively are defined as

$$z_1(t) \triangleq \left[e_1^T(t) \quad e_2^T(t) \quad r_1^T(t) \right]^T \tag{29}$$

$$z_2(t) \triangleq \left[e_3^T(t) \quad e_4^T(t) \quad r_2^T(t) \right]^T. \tag{30}$$

Assumption 3: The desired trajectory $X_{1d}(t)$ is sufficiently smooth and is bounded in the sense that $X_{1d}(t) \in \mathcal{L}_\infty \; \forall \; t \ge 0$.

1) Closed-Loop Error System: Based on the open-loop error system dynamics in (23), the control term $u_2(t)$ is designed as:

$$\dot{u}_2(t) = -k_{u2}\|u_2(t)\|sgn(r_2) - (k_{s2}+1)r_2 - \beta_2 sgn(r_2), \quad (31)$$

where $k_{u2}, k_{s2}, \beta_2 \in \mathbb{R}$ are positive, control gains.

After substituting (31) into (24), the closed-loop error dynamics is obtained as

$$\dot{r}_2 = \tilde{N}_2 + N_{2d} - k_{u2}\|u_2(t)\|sgn(r_2) - (k_{s2}+1)r_2 - \beta sgn(r_2) + \dot{\Delta}_g(t)u_2(t) - e_4. \quad (32)$$

Condition 1 (Gain): The control gains defined in (16) and (31) are selected according to the condition

$$k_{s1} > \frac{\rho^2(\|z_1\|)}{4min\{(\alpha_1 - \frac{1}{2}), (\alpha_2 - \frac{1}{2}), 1\}}, \quad (33)$$

$$k_{s2} > \frac{\rho^2(\|z_2\|)}{4min\{(\alpha_3 - \frac{1}{2}), (\alpha_4 - \frac{1}{2}), 1\}}, \quad (34)$$

$$k_{u1} \geq \epsilon_1, \quad \beta_1 \geq \zeta_{N_{1d}}, \quad k_{u2} \geq \epsilon_2, \quad \beta_2 \geq \zeta_{N_{2d}}. \quad (35)$$

IV. Stability Analysis

Theorem 1: For a given sufficiently smooth trajectory command X_{1d} and ψ_d, the quadrotor dynamics defined in (3-6), along with the control law defined in (16) and (31) ensures that all the system signals remain bounded throughout the closed-loop operation and the tracking error is asymptotically regulated in the sense that

$$\|e(t)\| \to 0 \quad \text{for} \quad t \geq t_n < \infty, \quad (36)$$

where $t_n \in \mathcal{L}_\infty$ and provided the control gains defined in (16) and (31) are selected according to condition 1.

Remark 1 (Stability Analysis of Nonsmooth Systems): The following Lyapunov-based stability analysis does not include a rigorous treatment to address the discontinuous right hand side of the closed-loop error system in (17) and (32) (i.e., using Filippov solutions [25]). Note that this does not invalidate the current result, since the letter in [26] provides detailed Filippov solutions in a Lyapunov-based framework for a closed-loop system in a form similar to that in (17) and (32).

Proof: Let $V(z,t) : \mathbb{R}^{6n} \times [0,\infty) \to R$ be a non-negative function defined as

$$V = \frac{1}{2}e_1^T e_1 + \frac{1}{2}e_2^T e_2 + \frac{1}{2}e_3^T e_3 + \frac{1}{2}e_4^T e_4 + \frac{1}{2}r_1^T r_1 + \frac{1}{2}r_2^T r_2, \quad (37)$$

where $z(t) \in \mathbb{R}^{6n}$ is defined as

$$z(t) \triangleq \begin{bmatrix} z_1^T(t) & z_2^T(t) \end{bmatrix}^T. \quad (38)$$

After taking the time derivative of (37) and using (11), (17), (22), (32) along with the bounding inequalities in (27) and (28), the expression in (37) can be upper bounded as

$$\begin{aligned}\dot{V} \leq\ & e_1^T e_2 + e_3^T e_4 - \alpha_1\|e_1\|^2 - \alpha_2\|e_2\|^2 - \alpha_3\|e_3\|^2 \\ & - \alpha_4\|e_4\|^2 + \|r_1\|\rho(\|z_1\|)\|z_1\| + \|r_1\|\zeta_{N_{1d}} \\ & - \|r_1\|(k_{u1})\|u_1\| - (k_{s1}+1)\|r_1\|^2 - \beta_1\|r_1\| + \epsilon_1\|r_1\|\|u_1\| \\ & + \|r_2\|\rho(\|z_2\|)\|z_2\| + \|r_2\|\zeta_{N_{2d}} - \|r_2\|(k_{u2})\|u_2\| \\ & - (k_{s2}+1)\|r_2\|^2 - \beta_2\|r_2\|\epsilon_2\|r_2\|\|u_2\|. \end{aligned} \quad (39)$$

But $e_1^T e_2$ and $e_3^T e_4$ can be upper bounded as

$$e_1^T e_2 \leq \frac{1}{2}\|e_1\|^2 + \frac{1}{2}\|e_2\|^2; \quad e_3^T e_4 \leq \frac{1}{2}\|e_3\|^2 + \frac{1}{2}\|e_4\|^2. \quad (40)$$

By using (40), and the gains k_{u1}, k_{u2}, β_1 and β_2 satisfy the gain condition in (35), the upper bound in (39) can be further simplified as

$$\begin{aligned}\dot{V}(z,t) \leq\ & -(\alpha_1 - \frac{1}{2})\|e_1\|^2 - (\alpha_2 - \frac{1}{2})\|e_2\|^2 - \|r_1\|^2 \\ & - k_{s1}\left[\|r_1\| - \frac{\rho(\|z_1\|)}{2k_{s1}}\|z_1\|\right]^2 + \frac{\rho^2(\|z_1\|)}{4k_{s1}}\|z_1\|^2 \\ & - (\alpha_3 - \frac{1}{2})\|e_3\|^2 - (\alpha_4 - \frac{1}{2})\|e_4\|^2 - \|r_2\|^2 \\ & - k_{s2}\left[\|r_2\| - \frac{\rho(\|z_2\|)}{2k_{s2}}\|z_2\|\right]^2 + \frac{\rho^2(\|z_2\|)}{4k_{s2}}\|z_2\|^2, \end{aligned} \quad (41)$$

$$\dot{V}(z,t) \leq -\left[min\{\eta_1, \eta_2\} - \frac{\rho^2(\|z\|)}{4min\{k_{s1}, k_{s2}\}}\right]\|z\|^2, \quad (42)$$

where $\eta_1 \triangleq min\{(\alpha_1 - \frac{1}{2}), (\alpha_2 - \frac{1}{2}), 1\}$ and $\eta_2 \triangleq min\{(\alpha_3 - \frac{1}{2}), (\alpha_4 - \frac{1}{2}), 1\}$. Provided the gain condition in (33) and (34) are satisfied, (37) and (42) can be used to show that $V(t) \in \mathcal{L}_\infty$; hence, $e_1(t), e_2(t), e_3(t), e_4(t), r_1(t), r_2(t) \in \mathcal{L}_\infty$. Given that $e_1(t), e_2(t), e_3(t), e_4(t), r_1(t), r_2(t) \in \mathcal{L}_\infty$, a standard linear analysis technique can be used along with (11) and (22) to show that $\dot{e}_1(t), \dot{e}_2(t), \dot{e}_3(t), \dot{e}_4(t) \in \mathcal{L}_\infty$. Since $e_1(t), e_2(t), e_3(t), e_4(t), \dot{e}_1(t), \dot{e}_2(t), \dot{e}_3(t), \dot{e}_4(t) \in \mathcal{L}_\infty$, (10) and (18) can be used along with the assumption that $x_d(t), \dot{x}_d(t) \in \mathcal{L}_\infty$ to prove that $x(t), \dot{x}(t) \in \mathcal{L}_\infty$. Given that $x(t), \dot{x}(t) \in \mathcal{L}_\infty$, (3-6) can be used along with the Assumption 1 to prove that the control input $u_1(t), u_2(t) \in \mathcal{L}_\infty$. Since $r_1(t), r_2(t) \in \mathcal{L}_\infty$, Assumption 1 can be used along with (16) and (31) to prove that $\dot{u}_1(t)$ and $\dot{u}_2(t) \in \mathcal{L}_\infty$.

The definition of $V(z,t)$ in (37) can be used along with the inequality (42) to show that $V(z,t)$ can be upper-bounded as

$$\dot{V}(z,t) \leq -cV(z,t), \quad (43)$$

provided the sufficient condition in (33) and (34) are satisfied. The differential inequality in (43) can be expressed as

$$V(z,t) \leq V(z(0))e^{-ct}. \quad (44)$$

Hence, (37),(38) and (43) can be used to conclude that

$$\|e(t)\| \leq \|z(0)\|e^{-\frac{c}{2}t} \qquad \forall \ t \in [0,\infty). \quad (45)$$

■

V. Simulation Results

A numerical simulation was created to test the performance of the proposed control structure. The simulation demonstrates the performance efficiency of the modified RISE-based (MRISE) control law in the outer loop (16) and inner loop (31) that compensates for parametric uncertainties and disturbances. The control law also tracks predefined 3D trajectories of varying speeds. The modified RISE-based control law achieves desired tracking performance in the presence of uncertainties and disturbances. In the numerical implementation of the control law presented here, the discontinuous

TABLE I
PHYSICAL PARAMETERS

Parameter	Description	Value
m	Mass of the Quadrotor	2 kg
g	Acceleration due to Gravity	9.81 ms^{-2}
l	Distance from rotor to center of mass	0.4 m
c	Force-to-moment factor	0.05
J	Moment of Inertia Matrix	diag(0.16,0.16,0.32) kgm^2
K_1,K_2	Damping Matrices	diag(0.01,0.01,0.01) Nms^2; diag(0.012,0.012,0.012) Nms^2

signum function is replaced with the continuously differentiable tanh() function. This is a standard approximation, which relates to the well-accepted definition of an equivalent value operator of a discontinuous function [27]. The use of tanh(·), detracts in no way from the validity of the stability analysis presented in the letter.

The physical parameters of the quadrotor are given in Tab. I and the initial conditions for the quadrotor are set to zero. The considered parametric uncertainties and external disturbances acting on the dynamics of the quadrotor are given as:

$$m_\Delta = unc * m, \quad J_\Delta = unc * J, \quad \Delta l = unc * l,$$
$$\Delta c = unc * c, \quad K_{1\Delta} = unc * \bar{K}_1, \quad K_{2\Delta} = unc * \bar{K}_2$$
$$\left[d_\Lambda\right] = i * \left[s(t), c(t), s(t)c(t))\right]^T,$$
$$\left[d_\Gamma\right] = i * \left[s(0.5t), c(0.5t), s(0.5t)c(0.5t))\right]^T$$

where $s(\cdot)$, $c(\cdot)$ denotes $sin(\cdot)$ and $cos(\cdot)$ functions respectively. *unc* is the uncertainty associated with respective variables. The *unc* is varied from 0% to 30%. d_Λ and d_Γ are the disturbance magnitudes in the position and orientation loop axis respectively, where the disturbance magnitude i takes the values ranging between 1,. . ., 10. The disturbance is introduced at $t = 25$sec during the simulation. The choice of control gains presented in this letter provide closed-loop convergence upto an uncertainty of 30% and disturbance magnitude ranging between 1 and 10.

The control gains associated with the outer loop in (16) are given as $k_{u1} = 0.01$, $k_{s1}= 2$, $\beta_1 = 0.5$, $\alpha_1= 5$, $\alpha_2 = 2.5$; and those of the inner loop in (31) are given as $k_{u2} = 0.01$, $k_{s2}= 5$, $\beta_2 = 2$, $\alpha_3= 10$, $\alpha_4 = 9$, respectively. The desired trajectory is defined as

$$\left[x_{des}, y_{des}, z_{des}, \psi_{des}\right]^T = \left[4sin(t), 4cos(t), t, sin(t)\right]^T. \quad (46)$$

The simulations are performed in MATLAB *R*2019*b*, on a AMD Ryzen 9 3900x processor with 32Gigabytes of RAM. The simulation results are summarized in Fig. 1–4. The results show a comparison between traditional RISE-based control formulation in [24] and modified RISE-formulation presented in this letter. The comparison is for a specific case, with *unc* = 20% and the disturbance magnitude $i = 10$.

Fig. 1 shows the positional state x, y, z (red) of the quadrotor tracking using the control structure presented in this letter, is compared with the quadrotor trajectory (blue) using RISE-based control in [24] with the desired (black) trajectory defined in (46). The right portion of the Fig. 1 shows the corresponding errors associated with each state x, y, z. When the disturbance is introduced at $t = 25$sec, the proposed control structure reacted more robustly there by reducing the

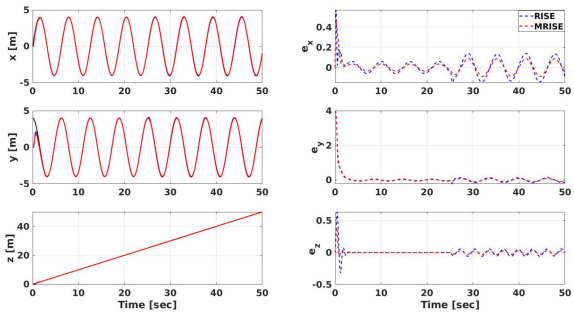

Fig. 1. [Left] Time evolution of the position of the quadrotor, [right] Error between the desired and current state.

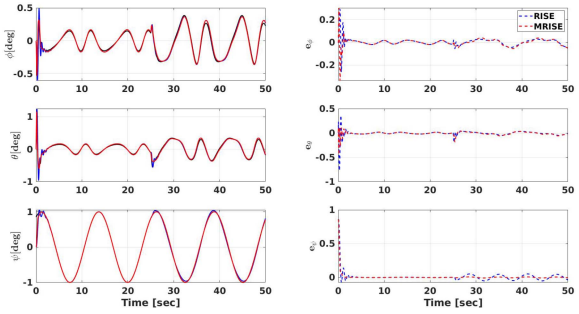

Fig. 2. [Left] Time evolution of the orientation of the quadrotor, [right] Error between the desired and current state.

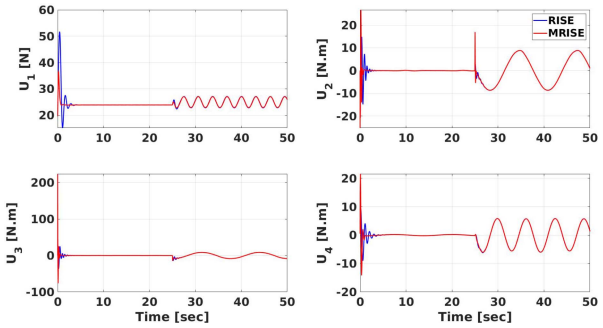

Fig. 3. Time Evolution of the control magnitudes during the closed loop operation.

error between the current and desired states. Fig. 2 shows the tracking of the desired orientation (black) and the quadrotor orientation using the proposed control method (red), along with the control method in [24] (blue). The right side of the Fig. 2 shows the corresponding error in the orientation (ϕ, θ, ψ)respectively.

Fig. 3 shows the time evolution of the control magnitudes during closed-loop operation. The magnitude of these control signals closely resemble the experimental results presented in [28] for trajectory tracking. Fig. 4 shows the bar graph of the mean RMS error in the states (X_1, X_2, X_3 and X_4) over varying uncertainty levels. Additional figures and a detailed proof of Theorem 1 are provided in the accompanying document with this letter. The results in Figs. 4 clearly demonstrate the improvement in the closed-loop performance that is achieved by the proposed modfied RISE-based control formulation that compensates under varying levels of uncertainty as well as disturbance magnitudes.

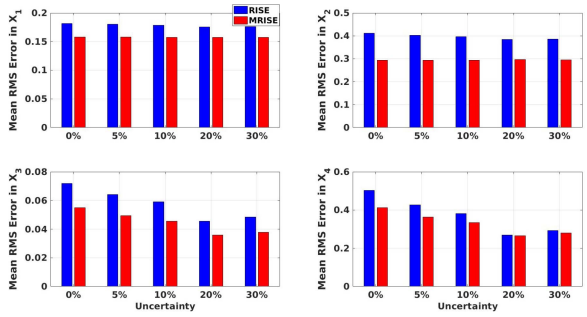

Fig. 4. Mean RMS Error during the closed-loop operation for the states X_1, X_2, X_3, X_4 with varying uncertainty levels.

VI. Conclusion

In this letter, a modified RISE state feedback controller is proposed which achieves asymptotic trajectory tracking of a quadrotor under parametric uncertainties and external disturbances. The modified RISE control is developed for both the position and the orientation loop. The advantages of the proposed control method is that it does not involve tedious gain tuning and the control algorithm tracks trajectories of varying speeds, uncertainties and disturbance magnitudes. A detailed theoretical Lyapunov-based stability analysis has been provided, which proves asymptotic regulation of both the outer loop and inner loop simultaneously. The effectiveness and advantages of the proposed control method are confirmed by numerical simulations, which paves a path to implement these control algorithms in a real world scenario. Future work will focus on including the effects of drag and other aerodynamic effects on the closed-loop performance and evaluating the proposed method through real-time experiments on a quadrotor UAV.

References

[1] S. Tang and V. Kumar, "Autonomous flight," *Annu. Rev. Control Robot. Autonom. Syst.*, vol. 1, pp. 29–52, May 2018.

[2] F. Kendoul, "Survey of advances in guidance, navigation, and control of unmanned rotorcraft systems," *J. Field Robot.*, vol. 29, no. 2, pp. 315–378, 2012.

[3] S. Bouabdallah, A. Noth, and R. Siegwart, "PID vs LQ control techniques applied to an indoor micro quadrotor," in *Proc. IEEE/RSJ Int. Conf. Intell. Robots Syst. (IROS)*, vol. 3, 2004, pp. 2451–2456.

[4] P. Pounds, R. Mahony, P. Hynes, and J. M. Roberts, "Design of a four-rotor aerial robot," in *Proc. Aust. Conf. Robot. Autom. (ACRA)*, 2002, pp. 145–150.

[5] Z. He and L. Zhao, "A simple attitude control of quadrotor helicopter based on Ziegler–Nichols rules for tuning PD parameters," *Sci. World J.*, vol. 2014, Dec. 2014, Art. no. 280180.

[6] P. Foehn and D. Scaramuzza, "Onboard state dependent LQR for agile quadrotors," in *Proc. IEEE Int. Conf. Robot. Autom. (ICRA)*, 2018, pp. 6566–6572.

[7] D. Lee, H. J. Kim, and S. Sastry, "Feedback linearization vs. adaptive sliding mode control for a quadrotor helicopter," *Int. J. Control Autom. Syst.*, vol. 7, no. 3, pp. 419–428, 2009.

[8] A. Mahmood and Y. Kim, "Decentrailized formation flight control of quadcopters using robust feedback linearization," *J. Franklin Inst.*, vol. 354, no. 2, pp. 852–871, 2017.

[9] N. Wang, S.-F. Su, M. Han, and W.-H. Chen, "Backpropagating constraints-based trajectory tracking control of a quadrotor with constrained actuator dynamics and complex unknowns," *IEEE Trans. Syst., Man, Cybern., Syst.*, vol. 49, no. 7, pp. 1322–1337, Jul. 2019.

[10] X. Shao, J. Liu, and H. Wang, "Robust back-stepping output feedback trajectory tracking for quadrotors via extended state observer and sigmoid tracking differentiator," *Mech. Syst. Signal Process.*, vol. 104, pp. 631–647, May 2018.

[11] A. Joukhadar, M. AlChehabi, C. Stöger, and A. Müller, "Trajectory tracking control of a quadcopter UAV using nonlinear control," in *Mechanism, Machine, Robotics and Mechatronics Sciences*. Cham, Switzerland: Springer, 2019, pp. 271–285.

[12] D. Cabecinhas, R. Cunha, and C. Silvestre, "A nonlinear quadrotor trajectory tracking controller with disturbance rejection," *Control Eng. Pract.*, vol. 26, pp. 1–10, May 2014.

[13] M. C. P. Santos, C. D. Rosales, J. A. Sarapura, M. Sarcinelli-Filho, and R. Carelli, "An adaptive dynamic controller for quadrotor to perform trajectory tracking tasks," *J. Intell. Robot. Syst.*, vol. 93, nos. 1–2, pp. 5–16, 2019.

[14] K. Wang, C. Hua, J. Chen, and M. Cai, "Dual-loop integral sliding mode control for robust trajectory tracking of a quadrotor," *Int. J. Syst. Sci.*, vol. 51, no. 2, pp. 203–216, 2020.

[15] N. Wang, Q. Deng, G. Xie, and X. Pan, "Hybrid finite-time trajectory tracking control of a quadrotor," *ISA Trans.*, vol. 90, pp. 278–286, Jul. 2019.

[16] U. Ansari, A. H. Bajodah, and M. T. Hamayun, "Quadrotor control via robust generalized dynamic inversion and adaptive non-singular terminal sliding mode," *Asian J. Control*, vol. 21, no. 3, pp. 1237–1249, 2019.

[17] B. Xian, D. M. Dawson, M. S. de Queiroz, and J. Chen, "A continuous asymptotic tracking control strategy for uncertain nonlinear systems," *IEEE Trans. Autom. Control*, vol. 49, no. 7, pp. 1206–1211, Jul. 2004.

[18] J. Shin, H. J. Kim, Y. Kim, and W. E. Dixon, "Autonomous flight of the rotorcraft-based UAV using RISE feedback and NN feedforward terms," *IEEE Trans. Control Syst. Technol.*, vol. 20, no. 5, pp. 1392–1399, Sep. 2012.

[19] H. Wang, X. Shao, J. Li, and J. Liu, "A velocity-free adaptive rise-based trajectory tracking approach for quadrotors with desired model compensation," *Aerosp. Sci. Technol.*, vol. 92, pp. 551–562, Sep. 2019.

[20] Z. Li, X. Ma, and Y. Li, "Robust tracking control strategy for a quadrotor using RPD-SMC and RISE," *Neurocomputing*, vol. 331, pp. 312–322, Feb. 2019.

[21] G. V. Raffo, M. G. Ortega, and F. R. Rubio, "An integral predictive/nonlinear H∞ control structure for a quadrotor helicopter," *Automatica*, vol. 46, no. 1, pp. 29–39, 2010.

[22] F. A. Goodarzi, D. Lee, and T. Lee, "Geometric nonlinear PID control of a quadrotor UAV on SE (3)," in *Proc. Eur. Control Conf. (ECC)*, 2013, pp. 3845–3850.

[23] R. Mahony, V. Kumar, and P. Corke, "Multirotor aerial vehicles: Modeling, estimation, and control of quadrotor," *IEEE Robot. Autom. Mag.*, vol. 19, no. 3, pp. 20–32, Sep. 2012.

[24] X. Shao, Q. Meng, J. Liu, and H. Wang, "RISE and disturbance compensation based trajectory tracking control for a quadrotor UAV without velocity measurements," *Aerosp. Sci. Technol.*, vol. 74, pp. 145–159, Mar. 2018.

[25] A. F. Filippov, *Differential Equations With Discontinuous Righthand Sides: Control Systems*, vol. 18. Dordrecht, The Netherlands: Springer, 2013.

[26] N. Fischer, R. Kamalapurkar, and W. E. Dixon, "Lasalle–Yoshizawa corollaries for nonsmooth systems," *IEEE Trans. Autom. Control*, vol. 58, no. 9, pp. 2333–2338, Sep. 2013.

[27] S. V. Drakunov, "Sliding-mode observers based on equivalent control method," in *Proc. 31st IEEE Conf. Decis. Control*, 1992, pp. 2368–2369.

[28] T. Huang, D. Huang, Z. Wang, and A. Shah, "Robust tracking control of a quadrotor UAV based on adaptive sliding mode controller," *Complexity*, vol. 2019, Dec. 2019, Art. no. 7931632.